Journal of the Korean Magnetic Resonance Society **2015**, *19*, 42-48

DOI 10.6564/JKMRS.2015.19.1.042

^{1}H, ^{15}N, and ^{13}C backbone assignments and secondary structure of the cytoplasmic domain A of mannitol trasporter $II^{Mannitol}$ from *Thermoanaerobacter Tencongensis* phosphotransferase system

Ko-On Lee and Jeong-Yong Suh*

Department of Agricultural Biotechnology, College of Agriculture and Life Sciences, Seoul National University, San 56-1, Shillim-Dong, Kwanak-Gu, Seoul 151-742, Korea

Received May 4, 2015; Revised May 21, 2015; Accepted June 03, 2015

Abstract The mannitol transporter Enzyme II^{Mtl} of the bacterial phosphotransferase system has two cytoplasmic phosphoryl transfer domains IIA^{Mtl} and IIB^{Mtl}. The two domains are linked by a flexible peptide linker in mesophilic bacterial strains, whereas they are expressed as separated domains in thermophilic strains. Here, we carried out backbone assignment of IIA^{Mtl} from thermophilic *Thermoanaerobacter Tencongensis* using a suite of heteronuclear triple resonance NMR spectroscopy. We have completed 94% of the backbone assignment, and obtained secondary structural information based on torsion angles derived from the chemical shifts. IIA^{Mtl} of *Thermoanaerobacter Tencongensis* is predicted to have six β strands and six α helices, which is analogous to IIA^{Mtl} of *Escherichia coli*.

Keywords Enzyme II^{Mtl}, mannitol transporter, phosphotransferase system, *Thermoanaerobacter Tencongensis*,

Introduction

The phosphoenolpyruvate phosphotransferase system (PTS)[1] represents a central bacterial signal transduction network for sugar uptake and phosphorylation. The initial step of PTS begins with Enzyme I autophosphorylation by PEP and subsequent phosphoryl transfer to the histidine phosphocarrier protein HPr, which is common to all downstream sugar-specific transporters Enzymes II. HPr carries over the phosphoryl group to Enzymes II that translocate and phosphorylate sugars. Domain construct of mannitol transfer Enzyme II^{Mtl} are highly conserved across species[1-3]. The mannitol transporter Enzyme II^{Mtl} is comprised of three domains; a transmembrane domain IIC^{Mtl} in the N terminus, followed by domain IIB^{Mtl} and IIA^{Mtl} in the C terminus, all of which are covalently connected as a single polypeptide in *Escherichia coli*[2-5]. In contrast, Enzyme II^{Mtl} of thermophilic *Thermoanaerobacter Tencongensis* is expressed as separated polypeptides IIA^{Mtl} and $IICB^{Mtl}$. Enzymes II^{Mtl} of *Escherichia coli* ($Ec II^{Mtl}$) and *Thermoanaerobacter Tencongensis* ($Tt II^{Mtl}$) display a high degree of sequence similarity (66% and 49% for sequence similarity and identity, respectively). Among the three domains, IIC^{Mtl} shows

* Address correspondence to: **Jeong-Yong Suh,** Department of Agricultural Biotechnology, College of Agriculture and Life Sciences, Seoul National University, San 56-1, Shillim-Dong, Kwanak-Gu, Seoul 151-742, Korea Tel: 82-2-880-4879; Fax: 82-2-877-4906; E-mail: jysuh@ snu.ac.kr

the highest sequence similarity, and IIA^{Mtl} shows the lowest similarity.

Within Enzyme II^{Mtl}, IIA^{Mtl} first accepts the phosphoryl group from HPr, and IIB^{Mtl} takes the phosphoryl group to the mannitol that is translocated through the cytoplasmic membrane by IIC^{Mtl1}. The crystal structure of the free *Ec*IIA^{Mtl6}, and the solution structures of the HPr:*Ec*IIA^{Mtl} complex[7] and the *Ec*IIA^{Mtl}:phosphoryl-*Ec*IIB^{Mtl} complex[8] has indicated that the structure of IIA^{Mtl} remains the same in its free and complex states, so that complex formation does not involve major conformational changes. The binding affinity between *Ec*IIA^{Mtl} and *Ec*IIA^{Mtl} is extremely weak (K_D = ~3.7 mM), but a flexible linker between the two domains confines the two domains within an effective distance of 46 Å, enabling a facile intramolecular domain association[8]. Given that the linker is absent in *Tt*II^{Mtl}, it is intriguing how *Tt*IIA^{Mtl} and *Tt*IIB^{Mtl} achieve the intermolecular interaction required for mannitol uptake. Differences in the interaction surface and/or side chain conformations might play a role to compensate the absence of the linker.

To understand the interaction between *Tt*IIA^{Mtl} and *Tt*IIB^{Mtl}, we carried out the backbone chemical shift assignment and obtained the secondary structure of *Tt*IIA^{Mtl} based on the backbone dihedral angles. This study will be useful to characterize the binding interface between *Tt*IIA^{Mtl} and *Tt*IIB^{Mtl}, which would compare with the interaction between the *Ec*IIA^{Mtl} and *Ec*IIB^{Mtl}.

Experimental Methods

Sample preparation- The gene *Tt*IIA^{Mtl} (1-146) was PCR-amplified from *Thermoanaer obacter Tencongensis* genomic. The PCR product was cloned into modified pET32a vector with a TEV cleavage site. The disulfide bonding residue, Cys-119, was mutated to Ala using the QuickChange kit (Agilent Technologies), and the new construct sequence was verified by DNA sequencing. The plasmid were introduced into *Escherichia coli strain BL21star(DE3) (Invitrogen) cell*s for expression. Cells were grown in minimal medium supplemented by ^{15}NH4Cl and ^{13}C6-glucose, induced with 1 mM isopropyl-D-thiogalactopyranoside at an *A600 of 0.7,* and harvested by centrifugation after overnight of induction. The cell pellet was resuspended in 50 ml (per liter of culture) of 20 mM Tris, pH 7.4, 200 mM NaCl and 1 mM phenylmethylsulfonyl fluoride. The suspension was lysed by three passages through Emulsiflex (Avestin, Canada) after homogenizing and centrifuged at 24,000*g for 20 min.* The supernatant fraction was filtered and loaded onto a HisTrap nickel-Sepharose column and the fusion protein was eluted with a 100-ml gradient of imidazole (10–500mM). The protein was then dialyzed against 50 mM Tris, pH 8.0, 4mM β-mercaptoethanol and digested with TEV protease. The cleaved His6tagwas removed by loading the digested proteins over a nickel-Sepharose column. Relevant fractions were purified by Superdex 75 gel filtration column (GE Healthcare) equilibrated with 20 mM Tris-HCl, pH 7.4, 200 mM NaCl and then on a monoQ anion exchange column (8ml; GE Healthcare) with a 160-ml gradient of 1M NaCl. NMR samples contained 1mM [U-15N/13C]-*Tt*IIA^{Mtl} (C119A) in 20mM Tris, pH 7.4 and 90% H_2O /10% D_2O.

NMR experiments and structure calculation and secondary structure prediction - NMR spectra were collected at 298K on Bruker AVANCE 900MHz spectrometers equipped with either a *z-shielded gradient triple resonance cryoprobe*. Spectra were processed using the NMRPipe program[9]and analyzed using the PIPP/CAPP/STAPP program[10] and NMRView[11]. Sequential assignment of ^{13}C, ^{15}N-labeled *Tt*IIA^{Mtl} protein was using 2D ^{15}N-HSQC spectrum and 3D triple resonance through-bond scalar correlation experiments (3D HNCO, HNCACO, HNCA, HN(CO)CA, HNCACB, CBCA(CO)NH experiments[12,13] Overall secondary structure and the backbone dihedral torsion angles were predicted from TALOS+[14] based on combined H_N, ^{15}N, Cα, Cβ and CO backbone chemical shifts.

Results and Discussion

Backbone assignments of TtIIA^{Mtl} - *Tt*IIA^{Mtl} consists of 146 amino acid residues with molecular weight of

16.4 kDa. The ^{1}H, ^{15}N and ^{13}C assignment obtained for *Tt*IIA^{Mtl} are listed in Table 1. Backbone assignments for amide resonances were obtained for 133 residues out of 141 residues (94%), excluding four proline residues and the N-terminal methionine. The 2D ^{1}H-^{15}N HSQC spectrum of *Tt*IIA^{Mtl} shows well dispersed amide resonances (Figure 1). The assignments are annotated with residue types and numbers in Figure 1. Six of the nine missing assignments are due to the absence of the corresponding amide resonances, and the remaining three residues were (Gly105, D106, E107) unassigned because of severe spectral overlap. In summary, 97% of Cα, 96% of Cβ and 95% of CO were assigned and listed in Table 1.

*Secondary structure of Tt*IIA^{Mtl} - Secondary structural information of *Tt*IIA^{Mtl} was calculated based on the $^{1}H_{N}$, ^{15}N, Cα, Cβ and CO chemical shift by using TALOS+ program based on the artificial neural network algorithm. The results of backbone torsion angles (φ, ψ) and the secondary structure are presented in Figure 2. The height of the bars reflects the probability of the secondary structure prediction. The secondary structure prediction showed that *Tt*IIA^{Mtl} is comprised of six β strands and six α-helices. Residue I11~L13 (β1), T53~Y55 (β2), V60~I62 (β3), I73~Y83 (β4), G86~D88 (β5) and R94~G103 (β6) constitute the β strands, and K20~E33 (α1), K39~E50 (α2), S67~K71 (α3), E107~A119 (α4), Y121~K130 (α5) and P134~K143 (α6) constitute the α-helices. *Ec*IIA^{Mtl} is composed of a central five-stranded beta sheet, flanked by five alpha helices[6-8]. Overall secondary structures of *Ec*IIA^{Mtl} and *Tt*IIA^{Mtl} are in good agreement, with a slight difference in the distribution of secondary structure elements. The β4 region of *Ec*IIA^{Mtl} is segmented into β4 and β5 of *Tt*IIA^{Mtl}. Notwithstanding, our data suggest that *Ec*IIA^{Mtl} and *Tt*IIA^{Mtl} would share a common backbone scaffold. Based on the current assignment, characterization of the binding interface between *Tt*IIA^{Mtl} and *Tt*IIB^{Mtl} is in progress.

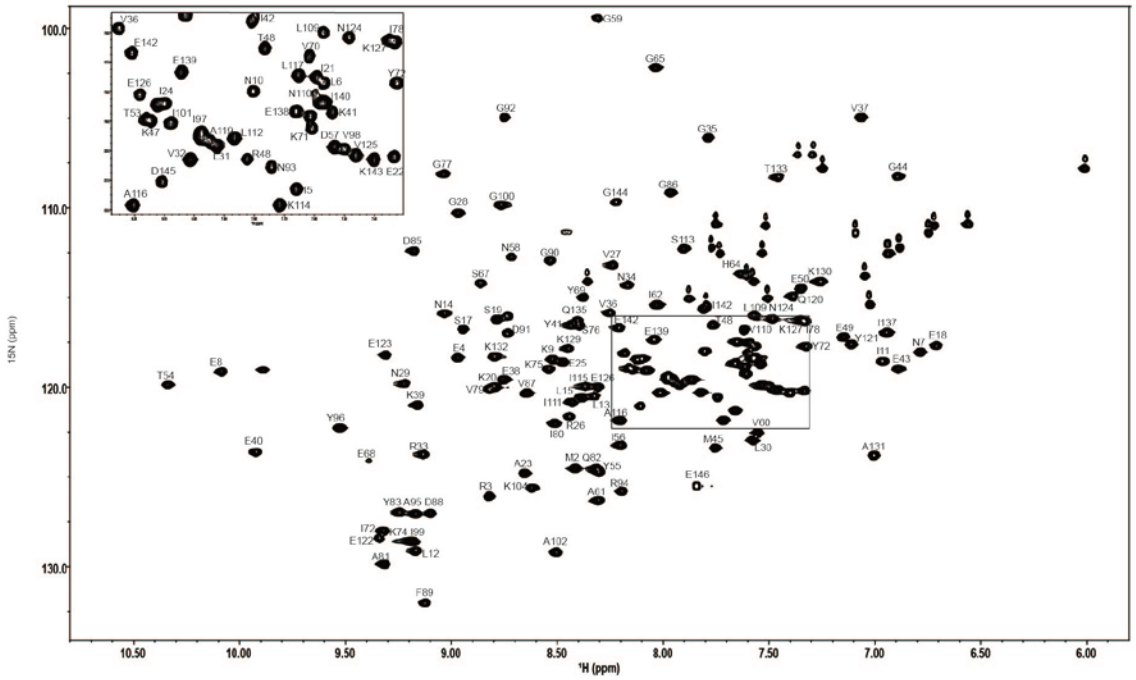

Figure 1. ^{1}H– ^{15}N HSQC spectra of *Tt*IIA^{mtl} annotated with the assignments obtained in this study.

Journal of the Korean Magnetic Resonance Society **2015**, *19*, 42-48

DOI 10.6564/JKMRS.2015.19.1.042

Table 1. Backbone HN, N, Cα, Cβ, CO chemical shifts of TtIIAmtl (unit:ppm)

Residue	HN	N	CA	CB	CO	Residue	HN	N	CA	CB	CO
1 MET			54.97	33.56	175.51	38 GLU	8.754	119.57	55.06	31.15	178.52
2 ASP	8.414	124.52	54.97	41.77	177.69	39 LYS	9.158	121.00	60.11	32.37	
3 ARG	8.823	126.08	56.74	29.69	177.93	40 GLU	9.923	123.62	60.77	27.07	177.86
4 GLU	8.970	118.35	58.64	29.30	178.72	41 TYR	8.436	116.54	62.59	40.02	176.96
5 ILE	7.659	121.30	63.10	39.08	174.03	42 ILE	7.809	115.64	65.66	37.59	178.35
6 LEU	7.569	117.77	54.18	44.32		43 GLU	6.890	118.97	59.06	28.79	178.42
7 ASN	6.790	118.05	51.91	40.78		44 GLY	6.893	108.24	45.60		176.17
8 GLU	10.084	119.14	60.66	28.94	177.20	45 MET	7.755	123.39	58.39	34.93	178.46
9 LYS	8.523	118.45	57.61	31.16	176.99	46 LYS	7.540	118.74	60.46	31.95	178.74
10 ASN	7.804	118.00	51.95	39.13	173.11	47 LYS	8.148	118.97	58.88	32.26	179.17
11 ILE	6.965	118.55	60.26	40.30	174.04	48 ARG	7.824	120.30	58.33	29.46	177.30
12 LEU	9.168	129.12	53.07	45.15	174.51	49 GLU	7.147	117.20	57.39	29.37	176.83
13 LEU	8.324	120.49	53.74	43.79	177.05	50 GLU	7.348	114.51	57.84	29.69	177.24
14 ASN	9.032	115.90	54.18	37.82	174.74	51 ASP	7.533	119.88	56.64	42.06	176.10
15 LEU	8.382	120.57	56.41	42.32	175.32	52 ILE	8.122	118.46	60.52	40.87	173.47
16 PRO			61.80	31.86	176.90	53 THR	8.148	118.97	62.24	69.10	174.35
17 SER	8.944	116.77	62.50	63.79	171.94	54 THR	10.338	119.87	62.48	68.53	175.96
18 GLU	6.711	117.67	53.38	29.86	174.25	55 TYR	8.301	124.76	60.14	39.18	175.94
19 SER	8.786	116.22	58.45	65.02	173.95	56 ILE	8.201	123.24	61.01		175.42
20 LYS	8.801	119.98	59.71	30.28	177.16	57 GLY			43.98		172.47
21 ILE	7.590	117.51	63.48	36.44	177.67	58 ASN	8.717	112.73	53.85	37.38	174.87
22 GLU	7.334	120.20	59.38	28.92	179.29	59 GLY	8.308	99.44	46.83		174.86
23 ALA	8.656	124.80	55.25	19.03	179.73	60 VAL	7.554	122.54	61.04	33.72	172.89
24 ILE	8.099	118.41	66.45	37.69	178.04	61 ALA	8.306	126.32	50.03	23.51	175.73
25 GLU	8.473	118.60	60.28	28.89	177.87	62 ILE	8.029	115.40	57.31	39.09	171.72
26 ARG	8.443	121.62	60.28	29.75	180.60	63 PRO			64.65	32.68	173.84
27 VAL	8.238	113.19	65.52	31.37	178.40	64 HIS	7.632	113.68	56.09	30.28	171.28
28 GLY	8.968	110.30	48.40		174.61	65 GLY	8.036	102.18	42.97		
29 ASN	9.219	119.79	56.36	38.05	178.01	66 VAL			59.92	35.14	176.12
30 LEU	7.574	122.96	57.62	41.75	178.73	67 SER	8.863	114.21	60.20	61.92	178.38
31 LEU	7.925	119.86	59.19	42.96	179.56	68 GLU	9.386	124.12	59.15	29.30	176.92

* Address correspondence to: **Jeong-Yong Suh,** Department of Agricultural Biotechnology, College of Agriculture and Life Sciences, Seoul National University, San 56-1, Shillim-Dong, Kwanak-Gu, Seoul 151-742, Korea Tel: 82-2-880-4879; Fax: 82-2-877-4906; E-mail: jysuh@ snu.ac.kr

32 VAL	8.013	120.31	64.88	32.31	180.95	69 TYR	8.376	114.98	60.73	37.40	177.22
33 ARG	9.132	123.74	59.42	29.70	178.37	70 VAL	7.616	116.80	64.89	30.88	178.23
34 ASN	8.166	114.30	52.49	37.18	175.00	71 LYS	7.608	119.27	57.51	30.80	176.43
35 GLY	7.788	106.10	46.10		174.31	72 TYR	7.324	117.72	57.53	38.78	173.78
36 VAL	8.251	115.85	61.48	38.86	176.63	73 ILE	9.321	128.01	61.42	33.69	174.04
37 GLU	7.064	104.96	57.30	36.27	175.46	74 LYS	9.185	128.60	58.14	32.66	177.02
75 LYS	8.540	118.99	55.30	35.49	172.90	111 ILE	8.430	120.84	65.87	38.41	177.46
76 SER	8.398	116.59	59.36	64.05	177.81	112 LEU	7.866	119.58	59.05	41.72	178.95
77 GLY	9.035	108.10	45.72		170.35	113 SER	7.904	112.28	61.55	62.77	176.53
78 ILE	7.347	116.24	59.32	42.35	173.78	114 LYS	7.717	121.85	59.15	32.27	179.69
79 VAL	8.817	120.13	58.76	35.29	174.70	115 ILE	8.368	119.95	63.17	35.92	177.43
80 ILE	8.511	122.01	60.71	41.50	172.03	116 ALA	8.203	121.85	55.49	17.68	179.95
81 ALA	9.315	129.86	50.16	22.28	174.03	117 LEU	7.652	117.46	57.79	41.69	179.79
82 GLN	8.313	124.55	54.54	33.96	172.12	118 THR	7.766	116.53	67.05	68.67	176.29
83 TYR	9.245	126.95		40.12	175.47	119 ALA	7.974	119.49	53.01	18.59	176.01
84 PRO			65.90	32.45	177.22	120 GLN	7.385	114.93	57.05	28.56	175.20
85 ASP	9.175	112.41	54.22	41.90	178.70	121 TYR	7.111	117.61	61.52	28.56	176.28
86 GLY	7.965	109.16	44.57		171.54	122 GLU	9.337	128.42	60.53	29.38	178.05
87 VAL	8.644	120.32	60.87	35.41	175.59	123 GLU	9.309	118.21	59.34		179.09
88 ASP	9.097	127.03	54.54	40.16	175.23	124 ASN	7.484	116.18	55.37	37.87	177.44
89 PHE	9.123	132.01	59.02	40.34	176.63	125 VAL	7.461	120.16	67.05	31.26	178.02
90 GLY	8.533	112.94	44.49		173.10	126 GLU	8.309	120.00	59.44	28.88	178.89
91 ASP	8.734	116.98	55.69	39.96	175.34	127 LYS	7.334	116.32	59.79	32.55	178.89
92 GLY	8.750	104.96	45.25		174.42	128 LEU	7.950	119.69	58.10	42.16	178.64
93 ASN	7.742	120.57	52.24	37.60	173.09	129 LYS	8.450	117.84	60.03	32.61	176.77
94 ARG	8.194	125.80	54.83	31.70	173.92	130 LYS	7.258	114.11	55.60	33.40	176.58
95 ALA	9.168	127.06	50.25	21.63	175.42	131 ALA	7.005	123.80	53.27	19.53	177.92
96 TYR	9.527	122.27	58.86	41.09	174.05	132 LYS	8.796	118.29	55.97	34.92	176.63
97 ILE	7.977	119.45	57.71	38.30	176.29	133 THR	7.456	108.30	57.94	70.49	173.13
98 VAL	7.500	119.93	62.67	38.38	175.09	134 PRO			65.32	32.56	177.81
99 ILE	9.183	128.60	59.48	39.34	175.93	135 GLN	8.403	116.28	59.77	27.12	177.81
100 GLY	8.765	109.86	44.80		173.11	136 GLU	7.613	118.86	59.25	30.80	178.77
101 ILE	8.078	119.05	59.65	42.85	175.01	137 ILE	6.945	116.95	63.86	36.62	176.70
102 ALA	8.505	129.20	52.15	22.33	173.46	138 ILE	7.661	118.67	66.34	37.85	176.97
103 GLY			43.89		170.96	139 GLU	8.043	117.35	59.39	29.52	179.27
104 LYS	8.621	125.62	55.57	33.19	177.26	140 ILE	7.571	118.37	64.25	38.01	178.30
105 GLY						141 LEU			57.42	41.68	
106 ASP						142 GLU	8.212	116.73	60.64	30.12	177.18
107 GLU						143 LYS	7.400	120.31	57.43	32.42	177.45
108 HIS			60.70	31.34	175.86	144 GLY	8.220	109.67	45.67	57.63	173.73

109 LEU	7.570	115.98	57.42	41.04	179.89	145 ASP	8.108	121.04	54.16	41.38	175.25
110 ASN	7.597	118.08	56.32	38.17	177.72	146 GLU	7.843	125.51	58.23	31.08	

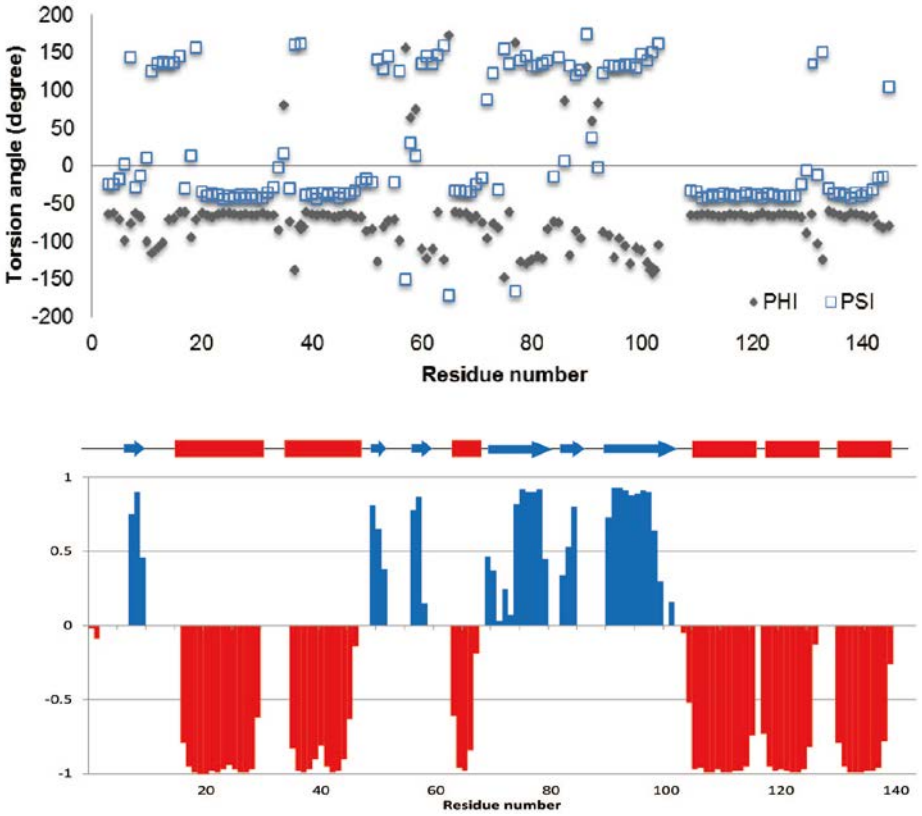

Figure 2. Summary of the backbone torsion angle and the secondary structure *Tt*IIA$^{mtl.}$ Backbone torsion angles(ϕ, ψ) were predicted using TALOS+ with backbone chemical shifts. Filled diamond indicated the phi (ϕ) and open square shows the psi (ψ), respectively in the upper panel. Predicted secondary structure (blue positive bar, beta-sheet; red negative bar, helix) for all residues are shown in the lower panel. The height of the bars reflects the probability of the neural network secondary structure prediction, and schematic representations of secondary structure is displayed above the prediction scores

Acknowledgements

This work was supported by a National Research Foundation of Korea (NRF) grant (2013R1A1A2010856). The authors thank the high field NMR facility at the Korea Basic Science Institute and the National Center for Inter-university Research Facilities.

References

1. P. W. Postma, J. W. Lengeler, G. R. Jacobson, *in* "Escherichia coli and Salmonella: Cellular and Molecular Biology" (Neidhardt, F. C., Eds.). pp.1149. American Society for Microbiology Press, Washington D. C., 1996.
2. G. T. Robillard, J. Broos, *Biochim. Biophys. Acta.* **1422**, 73 (1999)
3. Tchieu, J.H., Norris, V, Edwards, JS, Saier, M.H., *J. Mol. Microbiol.Biotechnol.* **3**, 329 (2001)
4. R. P. Van Weeghel, G. H. Meyer, H. H. Pas, W. Keck, G. T. Robillard, *Biochemistry.* **30**, 9478 (1991)
5. J.S. Lolkema, H. Kuiper, R. H. ten Hoeve-Duurkens, G. T. Robillard, *Biochemistry.* **32**, 1396 (1993)
6. R.L. van Montfort, T. Pijning, K.H. Kalk, I. Hangyi, M. L. Kouwijzer, G. T. Robillard, B. W. Dijkstra, *Structure*. **6**, 377 (1998)
7. G. Cornilescu, B. R. Lee, C.C. Cornilescu, G. Wang, A. Peterkofsky, G. M. Clore, *J Biol Chem*, **277**, 42289 (2002)
8. J. Y. Suh, M. Cai, D. C. Williams, G. M. Clore, *J Biol Chem*. **281**, 8939 (2006)
9. F. Delaglio, S. Grzesiek, G. W. Vuister, G. Zhu , J. Pfeifer, A. Bax, *J Biomol NMR.* **6**, 277 (1995)
10. D. S. Garrett, R. Powers, A. M. Gronenborn, G. M. Clore, *J. Magn. Reson.* **95**, 214 (1991)
11. B. A. Johnson, R. A. Blevins, *J Biomol NMR* **4**, 603, (1994)
12. S.Y. Kwak,W. H. Lee, J. Shin, S. G. Ko, W. T. Lee, *J. Kor. Magn. Reson. Soc.* **11**, 73 (2007)
13. K. Y. Lee, S. J. Kang, Y. J. Bae, K. Y. Lee, J. H. Kim, I. Lee, B. J. Lee, *J. kKr. Magn. Reson. Soc.* **17**,105 (2013)
14. Y. Shen, F. Delaglio, G. Cornilescu, A. Bax , *J. Biomol. NMR*, **44**, 213 (2009)